

Open Research Online

The Open University's repository of research publications
and other research outputs

Stress suppresses and learning induces plasticity in CA3 of rat hippocampus: a three-dimensional ultrastructural study of thorny excrescences and their postsynaptic densities

Journal Item

How to cite:

Stewart, M. G.; Davies, H. A.; Sandi, C.; Kraev, I. V.; Rogachevsky, V. V.; Peddie, C. J.; Rodriguez, J. J.; Cordero, M. I.; Donohue, H. S.; Gabbott, P. L. and Popov, V. I. (2005). Stress suppresses and learning induces plasticity in CA3 of rat hippocampus: a three-dimensional ultrastructural study of thorny excrescences and their postsynaptic densities. *Neuroscience*, 131(1) pp. 43–54.

For guidance on citations see [FAQs](#).

© [\[not recorded\]](#)

Version: Version of Record

Link(s) to article on publisher's website:

<http://dx.doi.org/doi:10.1016/j.neuroscience.2004.10.031>

Copyright and Moral Rights for the articles on this site are retained by the individual authors and/or other copyright owners. For more information on Open Research Online's data [policy](#) on reuse of materials please consult the policies page.

STRESS SUPPRESSES AND LEARNING INDUCES PLASTICITY IN CA3 OF RAT HIPPOCAMPUS: A THREE-DIMENSIONAL ULTRASTRUCTURAL STUDY OF THORNY EXCRESCENCES AND THEIR POSTSYNAPTIC DENSITIES

M. G. STEWART,^{a,*} H. A. DAVIES,^a C. SANDI,^c
I. V. KRAEV,^b V. V. ROGACHEVSKY,^b C. J. PEDDIE,^a
J. J. RODRIGUEZ,^a M. I. CORDERO,^{a,c} H. S. DONOHUE,^a
P. L. A. GABBOTT^a AND V. I. POPOV^{a,b}

^aDepartment of Biological Sciences, The Open University, Walton Hall, Milton Keynes MK7 6AA, UK

^bInstitute of Cell Biophysics, Russian Academy of Sciences, Pushchino 142290, Russia

^cLaboratory of Behavioral Genetics, Brain Mind Institute, Ecole Polytechnique Federale de Lausanne, CH-1015 Lausanne, Switzerland

Abstract—Chronic stress and spatial training have been proposed to affect hippocampal structure and function in opposite ways. Previous morphological studies that addressed structural changes after chronic restraint stress and spatial training were based on two-dimensional morphometry which does not allow a complete morphometric characterisation of synaptic features. Here, for the first time in such studies, we examined these issues by using three-dimensional (3-D) reconstructions of electron microscope images taken from thorny excrescences of hippocampal CA3 pyramidal cells. Ultrastructural alterations in postsynaptic densities (PSDs) of thorny excrescences receiving input from mossy fibre boutons were also determined, as were changes in numbers of multivesicular bodies (endosome-like structures) within thorny excrescences and dendrites. Quantitative 3-D data demonstrated retraction of thorny excrescences after chronic restraint stress which was reversed after water maze training, whilst water maze training alone increased thorny excrescence volume and number of thorns per thorny excrescence. PSD surface area was unaffected by restraint stress but water maze training increased both number and area of PSDs per thorny excrescence. In restrained rats that were water maze trained PSD volume and surface area increased significantly. The proportion of perforated PSDs almost doubled after water maze training and restraint stress. Numbers of endosome-like structures in thorny excrescences decreased after restraint stress and increased after water maze training. These findings demonstrate that circuits involving contacts between mossy fibre terminals and CA3 pyramidal cells at stratum lucidum level are affected conversely by water maze training and chronic stress, confirming the remarkable plasticity of CA3 dendrites. They provide a clear illustration of the structural modifications that occur after life experiences noted for their different impact on hip-

poampal function. © 2005 Published by Elsevier Ltd on behalf of IBRO.

Key words: stress, water maze training, dendritic spines, PSDs, endosomes.

The hippocampus shows remarkable synaptic plasticity in response to a variety of experimental paradigms including long term potentiation (Bliss and Collingridge, 1993) and learning models, of which spatial training in a Morris water maze has been amongst the most intensively investigated (O'Keefe and Nadel, 1978; Morris et al., 1982; Riedel et al., 1999; Eyre et al., 2003). Chronic restraint stress also causes alterations in biochemistry, pharmacology and morphology within the hippocampus, especially in CA1 and CA3 (Magariños and McEwen, 1995; de Kloet et al., 1998; McEwen, 1999; Venero et al., 2002), and cognitive alterations have been systematically reported after repeated exposure to stress (Conrad et al., 1996; McEwen, 1999; Fuchs et al., 2001; Sandi et al., 2001, 2003; Cordero et al., 2003).

Changes in synaptic and dendritic structure are believed to underlie synaptic plasticity in the hippocampus (Moser et al., 1994, 1997; Stewart et al., 2000; O'Malley et al., 2000; Nikonenko et al., 2002; Eyre et al., 2003; Muller and Nikonenko, 2003; Harris et al., 2003; Mezey et al., 2004; Popov et al., 2004). In rats stressed for 3–4 weeks, synaptic changes occur in CA3, including alterations in mossy fibre terminals (Magariños et al., 1997), a loss of synapses and a reduction in the surface area of postsynaptic densities (Sousa et al., 2000). In contrast overtraining rats in a water maze during 3 consecutive days increases mossy fibre terminal density in CA3 stratum oriens, when evaluated 9 or 30 days after training (Ramírez-Amaya et al., 1999, 2001).

We have shown previously that exposure to chronic restraint stress for 21 days induces a loss of simple unperforated synapses in stratum lucidum of CA3, whilst spatial learning reverses this effect (Sandi et al., 2003). Our study was based upon unbiased stereological methods (Sterio, 1984) where three-dimensional (3-D) estimations were derived from 2-D parameters. Such an approach permits neither a precise evaluation of changes in morphometric parameters of postsynaptic density (PSD) size and shape, nor details of alterations in spine morphology. Whilst two-photon imaging techniques have proven attractive to study hippocampal spines in slices (Nikonenko et al., 2002; En-

*Corresponding author. Tel: +44-1908-653448; fax: +44-1908-654167. E-mail address: m.g.stewart@open.ac.uk (M. G. Stewart).

Abbreviations: ANOVA, analysis of variance; DG, dentate gyrus; ER, endoplasmic reticulum; MFB, mossy fibre boutons; MVB, multivesicular body/endosomes; NCAM, neural cell adhesion molecule; PB, phosphate buffer; PFA, paraformaldehyde; PSD, postsynaptic density; rER, cisterns of rough endoplasmic reticulum; TE, thorny excrescences; 3-D, three-dimensional.

gert and Bonhoeffer, 1999), their optical resolution does not permit examination of the morphology of synaptic contacts. The shape and size of synapses and their spatial relationships with dendritic spines and shafts can only be ascertained from 3-D reconstructions of serial ultrathin sections (Fiala and Harris, 2001). Chicurel and Harris (1992) described the 3-D form and internal structure of CA3 branched dendritic spines and their synaptic relationships with mossy fibre boutons (MFB) in the hippocampus of normal rats.

Here we have used serial ultrathin sectioning and 3-D reconstruction to evaluate the structural effects of exposure to chronic restraint stress and/or training in a hippocampus-dependent water maze task on specific synaptic connexions in dorsal CA3 of the hippocampus, a region strategically involved in spatial learning (Jung et al., 1994; Moser et al., 1993, 1995). Alterations in the 3-D structure of dendritic segments, thorny excrescences (TE) and postsynaptic densities were examined in the stratum lucidum of CA3.

EXPERIMENTAL PROCEDURES

Experimental animals

All animal experimentation was performed exactly as described previously (Sandi et al., 2001, 2003) except that for electron microscopic studies the primary fixation regimen consisted of a paraformaldehyde (PFA)/glutaraldehyde mixture in 0.1 M Na cacodylate buffer (as described below). Briefly the details are as follows. Male Wistar rats (Harlan Iberica, Spain), were housed in groups of three per cage, under temperature ($22 \pm 2^\circ\text{C}$) and light (12-h light/dark cycle; lights on at 07:00 h) with free access to food and water in a colony room. Rats weighed 250 ± 25 g, at the commencement of the chronic stress procedure (for those animals assigned to the stress groups). Body weights were recorded periodically. In addition, rats were handled daily during the 3 days before the experiments. All efforts were made to minimise both the suffering and the number of animals used. Animal care procedures were conducted in accordance with the guidelines set by the European Community Council Directives (86/609/EEC).

Chronic stress procedure

Rats were subjected to chronic restraint stress for 21 days. The sessions consisted of 6 h/day (always between 8:00 a.m. and 2:00 p.m.) restraint of the animals in rat plastic restrainers (Cibertec, Spain) secured at the head and tail ends with clips. During the restraint sessions, the rats were individually placed, in independent plastic compartments, in a room adjacent to their colony. Therefore, the stress procedure used, in addition to the actual restraint, involved the daily handling and transportation of animals to a novel environment, two manipulations that can also be considered additional stressors. Each day, at the termination of the stress session, they were returned to their home cages. During this period, control animals were left undisturbed in the home cages. In the colony room, control and stressed rats were allocated in separate locations, on opposite walls. After termination of the last stress episode, rats were treated further (as described below) before intracardiac perfusion on day 23 (from the beginning of stress treatment). Four groups of rats were analysed in our experiments (all perfused approximately at a similar time after the commencement of the experimental period for the restraint stressed groups):

(A) Undisturbed rats (control, $n=4$), which were handled daily but subject neither to stress nor water maze training.

(B) Water maze only-trained rats ($n=4$), which were trained, as described below, on a learning acquisition session (eight trials) followed, 24 h later, by a reversal learning session (four trials), and perfused 15 min afterward.

(C) Restraint-stressed rats ($n=4$), which were stressed for 21 days, as described above, and perfused on the second day after the end of the stress period.

(D) Restraint-stressed rats plus water maze rats ($n=4$), which were restraint stressed as in C, then 24 h after the end of the stress period, trained in a water maze as in B, and perfused 15 min afterward.

Water maze learning

The Morris water maze used in our study was a black circular pool (2 m diameter, 45 cm high) filled with water (30 cm depth) at $24 \pm 1^\circ\text{C}$. The pool was divided into four quadrants of equal size. An invisible escape platform (11 cm diameter) was placed in the middle of one of the quadrants (1.5 cm below the water surface) equidistant from the side wall and middle of the pool. The behaviour of the animal (latency, distance and swim speed) was monitored by a video camera, mounted in the ceiling above the centre of the pool, and a computerised tracking system (Ethovision 1.90; Noldus IT, The Netherlands). Four different starting positions were equally spaced around the perimeter of the pool. The training session consisted of one massed session of eight training trials which were started from one of the four start positions, used in a random sequence equal for every rat. A trial began by placing the rat into the water facing the wall of the pool at one of the starting points. If a rat failed to escape within 120 s, it was guided to the platform by the experimenter. Once the rat reached the platform, it was allowed to remain for 30 s and then placed in a holding cage for an inter-trial interval of 30 s. After the last trial, the rats were dried off by placing them in a holding cage for 30 min, in a room heated to 28°C . There was always at least one companion rat (from the home cage) in the holding cage to avoid any isolation stress. Subsequently, they were returned to their home cages. Twenty-four hours afterward, rats were submitted to a reversal learning protocol, with the platform located in the quadrant opposite to the one used during the training session, and the procedure remained the same as for the spatial training phase. The rationale for performing a reversal learning task on the second training day was discussed previously (Sandi et al., 2003) and was to provide the rats with a new spatial learning challenge, which would allow us to examine structural correlates of the immediate preceding learning experience.

Tissue preparation and processing for ultrastructural microscopy

Fifteen minutes after either completing reversal learning, or after being handled (depending on the group to which they had been assigned), the rats were deeply anaesthetised with sodium pentobarbital (100 mg/kg, i.p.). Four rats from each experimental group were perfused transcardially with 100 ml of physiological saline, followed by 100 ml of 3% PFA and 0.5% glutaraldehyde in 0.1 M Na-cacodylate buffer (pH 7.2–7.4) at room temperature. Immediately after perfusion the brains were removed and 150 μm thick sections cut. Further fixation was made by immersion of slices in 2% glutaraldehyde–PFA in 0.1 M Na-cacodylate buffer for 24 h. The tissue was post-fixed with 1% osmium tetroxide and 0.01% potassium dichromate in the same buffer for 1–2 h at room temperature.

Tissue was dehydrated in graded aqueous solutions of ethanol from 40 to 96% (each for 10 min) and then 100% acetone (three changes, each for 10 min). Specimens were infiltrated with a mixture of 50% epoxy resin, 50% pure acetone for 30 min at room temperature. Each slice was placed on a Teflon support and covered with a capsule containing pure epoxy resin (Epon 812/

AralditeM epoxy resin) for 1 h at 60 °C and polymerised overnight at 80 °C. Slices in blocks were then coded and all further analyses were carried out with the investigator blind to the experimental status of the tissue.

The embedded slices on the block surface were trimmed with a glass knife along the entire surface of the hippocampal slice and 1–2 μm -thick sections cut. A trapezoid area was prepared with a glass knife, with one side of 20–25 μm in length, and included CA3 hippocampal area. The essential elements of the procedure are illustrated in Popov et al. (2004), except that here the area sectioned included CA3. Serial sections of grey-white colour (60–70 nm) were cut with a Diatome diamond knife and allowed to form a ribbon on the surface of a water/ethanol solution (2–5% ethanol in water) in the knife bath and were collected using Pioloform-coated slot copper grids. Sections were counterstained with saturated ethanolic uranyl acetate, followed by Reynolds (1963) lead citrate, and were then placed in a rotating grid holder to allow uniform orientation of sections on adjacent grids in the electron microscope.

Digital reconstructive analysis. Electron micrographs at a magnification of 6000 \times were obtained in a JEOL 1010 electron microscope from the CA3 stratum lucidum, at a distance of 10–20 μm from the layer of pyramidal cell bodies. Up to 160 serial sections per series were photographed to reconstruct an individual CA3 stratum lucidum dendritic segment, and a minimum of 10 segments were reconstructed per animal. A cross-sectioned myelinated axon, mitochondria, and dendrites spanning each section provided a fiducial reference for initial alignment of serial sections. Section thickness was determined using the approach of Fiala and Harris (2001) and was normally of 60–70 nm-thickness (grey-white colour). Digitally scanned EM negatives with a resolution of 900 dpi were aligned as JPEG images (software available from Drs. Fiala and Harris: <http://synapses.bu.edu>). Alignments were made with full-field images. Contours of individual dendritic segments with TE, axons, smooth and rough endoplasmic reticulum (ER), Golgi stacks/dictyosomes, PSDs, and mitochondria were traced digitally and volumes, areas, and total numbers of structures, were computed.

Parameters measured. The following quantitative measurements were computed directly from the 3-D reconstructed dendritic segments:

1. The volume of TE in μm^3
2. The surface area of TE in μm^2
3. The volume of PSDs in μm^3
4. Surface area of PSDs in μm^2
5. Proportion of perforated PSDs (as percentage of total)
6. Ratio of PSD area to TE area
7. Percentage occupation by PSDs of the TE surface area
8. The number of thorns per TE
9. The number of PSDs per TE
10. The number of multivesicular bodies (MVB; endosomes) per dendritic segment
11. The number of endosomes per TE

Statistical analysis. Micrococcal Origin software was used to graph, to obtain means and SDs, and to perform tests of significance, as described in the Results. Analyses of variance (ANOVAs) followed Tukey's unequal N honest significant differences tests were used. Data are presented as a mean \pm S.E. A one-way ANOVA was used for determination of significance which was set at $P < 0.05$.

Hippocampal volume

Because insufficient tissue was available from the ultrastructural studies to measure mean volumes in hippocampus a separate series of stress and water maze training experiments was per-

formed exactly as described above to provide four rats from each of the four experimental groups. The only difference was that the fixation mixture utilised acrolein instead of glutaraldehyde because the tissue was to be used additionally for immunocytochemistry experiments. Rats were perfused transcardially with 100 ml of physiological saline, followed by 50 ml of 3.75% acrolein in 2% PFA and in 0.1 M Na-phosphate buffer pH 7.4 (PB) followed by 200 ml of 2% PFA in PB. Immediately after perfusion the brains were removed and post-fixed overnight in 2% PFA in PB (pH 7.2–7.4) at 4 °C. Serial coronal sections (50 μm thick= t) were subsequently cut throughout the entire rostrocaudal extent of the hippocampi in the left and right hemispheres using a vibratome. The total number of sections and their order was noted. The volumes of the right dorsal anterior hippocampi in the different groups were estimated by using the Cavalieri method (Pakkenberg and Gundersen, 1997; Stuart and Oorschot, 1995). Dorsal anterior hippocampus is defined in the coronal plane, as extending from the rostral pole of the hippocampus (at approximately –1.6 mm posterior to Bregma; Swanson, 1998) to the region where the dorsal and ventral parts of the hippocampus become continuous (at approximately –4.3 mm posterior to Bregma).

From the complete rostrocaudal set of sections through the dorsal anterior hippocampus in each animal every fourth section (on average) in the series was mounted in order onto glass slides, air dried and subsequently stained with a solution of 0.1% Toluidine Blue in 0.1 M PB (pH 7.4) for 2 min. Sections were then washed, dehydrated in an ascending series of alcohols, passed through xylene and finally embedded in DPX. Sections were subsequently viewed and analysed at low magnification in a Nikon E600 digital photomicroscope.

Digital images including the hippocampus and surrounding structures were captured electronically and displayed on a computer screen (Fig. 1A). Using previously published cytoarchitectonic criteria (Swanson, 1998), the boundaries of hippocampal CA1, CA2 and CA3 subregions as well as the dentate gyrus (DG; including the polymorph cell layer) were defined in each rostrocaudal section of the right hemisphere (see Fig. 1), the hemisphere from which morphometric measurements were taken.

The mean surface areas of the hippocampal subregions under investigation (Fig. 1B) were then obtained using a calibrated measuring programme (Lucia Version 4.8; Laboratory Imaging Ltd., Prague, CZ). The total hippocampal, total CA3 and total DG volumes for the dorsal anterior hippocampus were then derived by multiplying the calculated mean surface area of each structure in each animal by the section thickness (t) and the total actual number of sections (n) in which the right dorsal anterior hippocampus appeared.

Data are presented as mean \pm standard deviation. Statistical comparisons in volume data between regions, hemispheres and animals were performed using multiple t -tests.

RESULTS

Behavioural analyses

Progressive learning was shown by both stressed and unstressed groups of rats, as indicated by a decrease in the distance to reach the hidden platform through the training trials (Fig. 2A). The data from the two sets of experiments, for ultrastructural studies and for volume measurement, were similar and have been combined in the Fig. 2. As previously found (Venero et al., 2002; Sandi et al., 2003), chronic restraint stress appeared to induce a slight impairment on acquisition in the water maze during the 'learning' session but here due to the low number of animals (a restriction related to the technical difficulties associated with 3-D studies), the differences were not

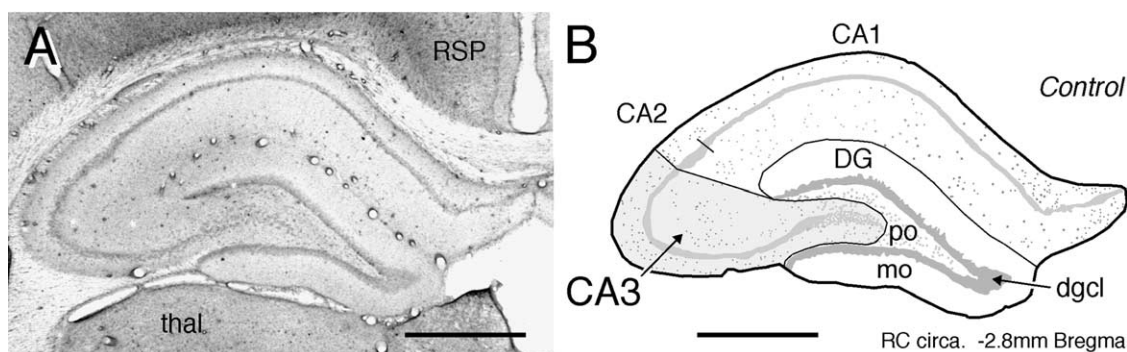


Fig. 1. Definition of hippocampal regions. (A) Toluidine Blue-stained section (50 μm thick) showing the dorsal anterior hippocampus in the right hemisphere of a control animal. Neighbouring regions are indicated (RSP, posterior retrosplenial cortex; thal, thalamus). Section viewed from anterior pole and taken along the rostrocaudal axis (RC) at approximately -2.8 mm from Bregma. (B) Line drawing of section shown in A indicating the perimeter boundary of the hippocampus, the CA1 and CA2 regions and the CA3 region (shaded). The DG is defined as composed of the molecular (mo) dentate granule cell layer (dgcl) and the polymorphic cell layer (po) of the hilus. Scale bars = 1 mm.

significant. No significant differences in performance were observed between stressed and unstressed rats when submitted to the 'reversal learning' task on the second water maze session (Fig. 2B).

Hippocampal volume

Mean volumes of dorsal anterior CA3, DG subregions and of total dorsal anterior hippocampus are shown in Table 1 for the four groups of rats, (i) control, (ii) stress, (iii) water maze only and (iv) stress plus water maze. There is a significant difference in volume for the total dorsal anterior hippocampus, due to a decrease in volume in stressed rats (14.5%, $P < 0.026$). However, there are no significant changes in the volume of either CA3 or DG in the dorsal anterior hippocampus in stressed rats compared with control or water maze-trained animals.

CA3 ultrastructure

Mossy fibres and TE were originally described by Ramón y Cajal (1911). Ultrastructurally, the stratum lucidum of the CA3 of all animals was characterised by the distinctive anatomical appearance of the giant boutons of mossy fibre axons (Sousa et al., 2000). TE are complex club like structures originating from the base of dendrites of CA3 pyramidal cells; they contain a thin stalk which is covered by small protrusions or thorns. Reconstructions were made of approximately 10 dendritic segments per animal from each of the experimental groups. The segments were reconstructed from a serial section series chosen at random in stratum lucidum, approximately 10–20 μm from the cell body. The location of typical TE can be seen by reference to Gonzales et al. (2001) who used horse radish peroxidase filling and 3-D reconstruction at light microscope level to examine the distribution of TE on CA3 pyramidal neurons.

Fig. 3A–D contains four consecutive sections from a series of 150 from the stratum lucidum of CA3c of a control rat which show one TE with thorns. Mossy fibre

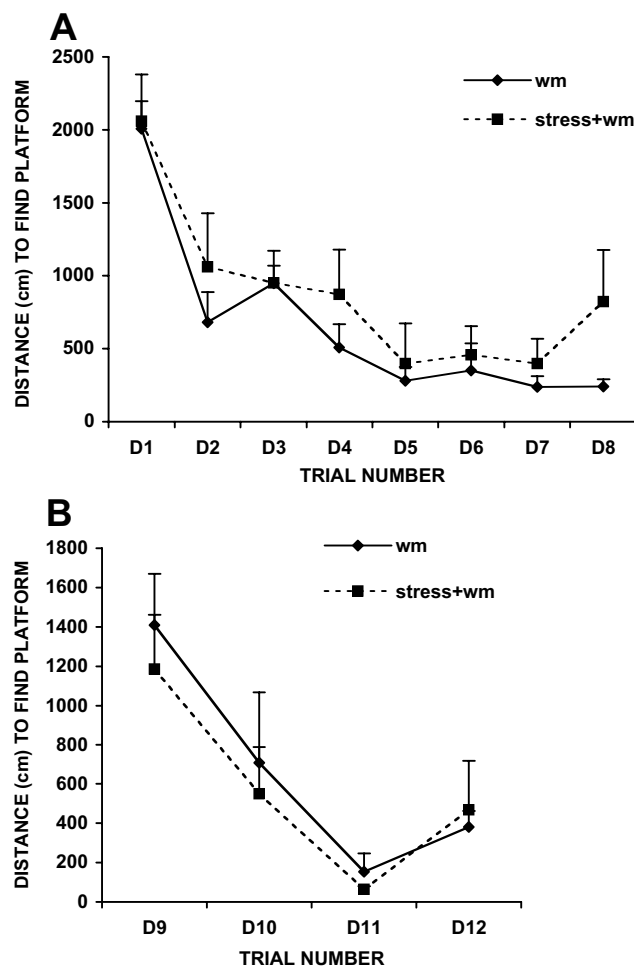


Fig. 2. Effect of chronic restraint stress on spatial learning in the water maze. The data show the mean distance (\pm S.E.M.; $n=8$ rats per group) travelled by rats to find the hidden platform in (A) a massed training session, of eight trials, D1–D8; and (B) a reversal learning session given 24 h afterward, D9–D12. Restraint stress induced a slight, though not significant, impairment of acquisition of spatial orientation, but did not affect performance in the reversal learning task.

Table 1. Stress is not associated with a change in the volume of dorsal anterior CA3 region^a

Animal group	DG volume, mm ³	CA3 volume, mm ³	Whole hippocampus volume, mm ³
Control	3.36±0.09	3.19±0.13	12.52±0.20*
Restraint	3.00±0.21	2.95±0.26	10.81±0.57*
Water maze	3.11±0.18	3.18±0.11	11.85±0.15
Restraint+water maze	3.06±0.13	3.19±0.14	11.92±0.20

^a Volume measurements were estimated by use of the Cavalieri method for the total hippocampus, DG and CA3 region of the right dorsal anterior hippocampus. (Values given as mean volumes±S.D. in mm³.) The boundaries of the CA1, CA2 and CA3 regions, as well as the DC (cell body layer, molecular layer and polymorphic cell layer) of the right dorsal anterior hippocampus are defined in Fig. 1B. (See text for details of the quantitative methodology). Statistical comparisons in volume data between regions, and animal groups were performed using multiple *t*-tests:

* Significant differences are present only between Control and Restraint for whole hippocampal hemisphere. There are no significant differences for either CA3 or dentate between stressed or control rats.

boutons (MFB) in Fig. 3A–D establish asymmetric synaptic contacts with the thorns and a dendrite. The thorn in Fig. 3A does not appear to contact with the dendrite in this micrograph though the beginnings of two separate spine protrusions are shown labelled TE. The spine protrusions are more apparent in consecutive sections, as shown in Fig. 3B and in Fig. 3C and 3D where the stem from the dendrite actually reaches the thorn. Higher power electron micrographs of Fig. 3B and Fig. 3C are presented in Fig. 3E and 3F which show detail of the two thorns. Cisterns of smooth endoplasmic reticulum (ER) and rough ER (rER) and MVB (endosome-like structures; Cooney et al., 2002), are clearly visible in Fig. 3E and 3F and the TE contains mitochondria and microtubules. There appears to be an extrusion from the postsynaptic membrane to the MVBs in the thorns in both Fig. 3E and 3F. Within thorns there are polyribosomes; cisterns of both smooth and rER (Fig. 3E, F).

Effect of restraint stress and water maze training on 3-D structure of CA3 dendritic segments

Three-dimensional reconstructions of approximately 10 dendritic segments in stratum lucidum (beginning 20 µm

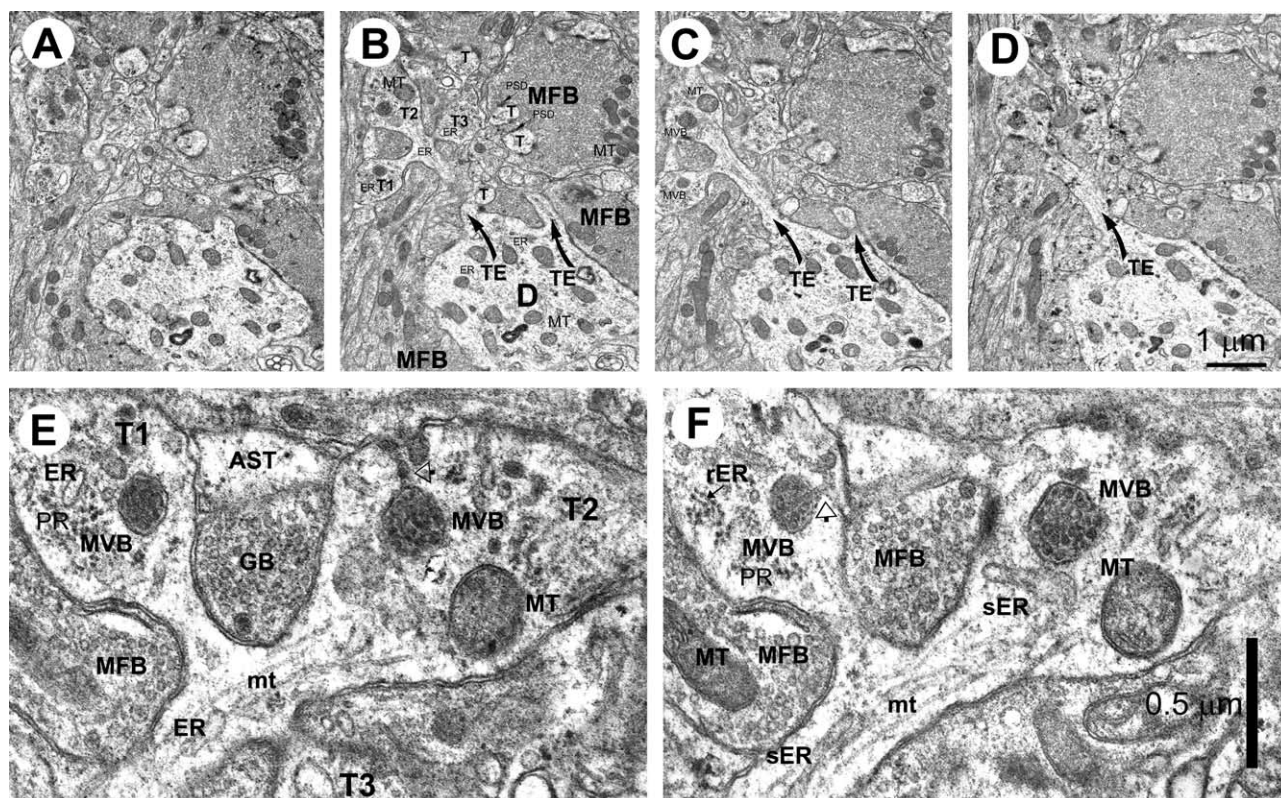


Fig. 3. (A–D) Four sections from a series of 150 from the stratum lucidum of CA3 of a control rat (approximately 15 µm from the cell body) which show large MFB, a dendrite (D), three thorns T1–T3 and TE. The TE are complex club like structures formed from the dendrites of CA3 pyramidal cells. MFB in A, B establish asymmetric synaptic contacts with the thorns and dendrite. The stalks of the TE in A do not appear to contact with the dendrite in this micrograph though the beginnings of two protrusions are shown labelled TE. The protrusions are more apparent in consecutive sections, as shown in B, and in C and D the stem from the dendrite actually reaches the thorns; scale bar=1 µm. (E, F) Higher power electron micrographs of B and C are presented in E and F and show detail of the two thorns. rER and MVBs (endosome-like structures) are clearly visible in E and F and polyribosomes (PR) are also present. (E) AST, astrocyte; GB, giant bouton. Open arrows in E and F show the fusion of endosome-like structures with post synaptic membrane of the TE; scale bar=0.5 µm.

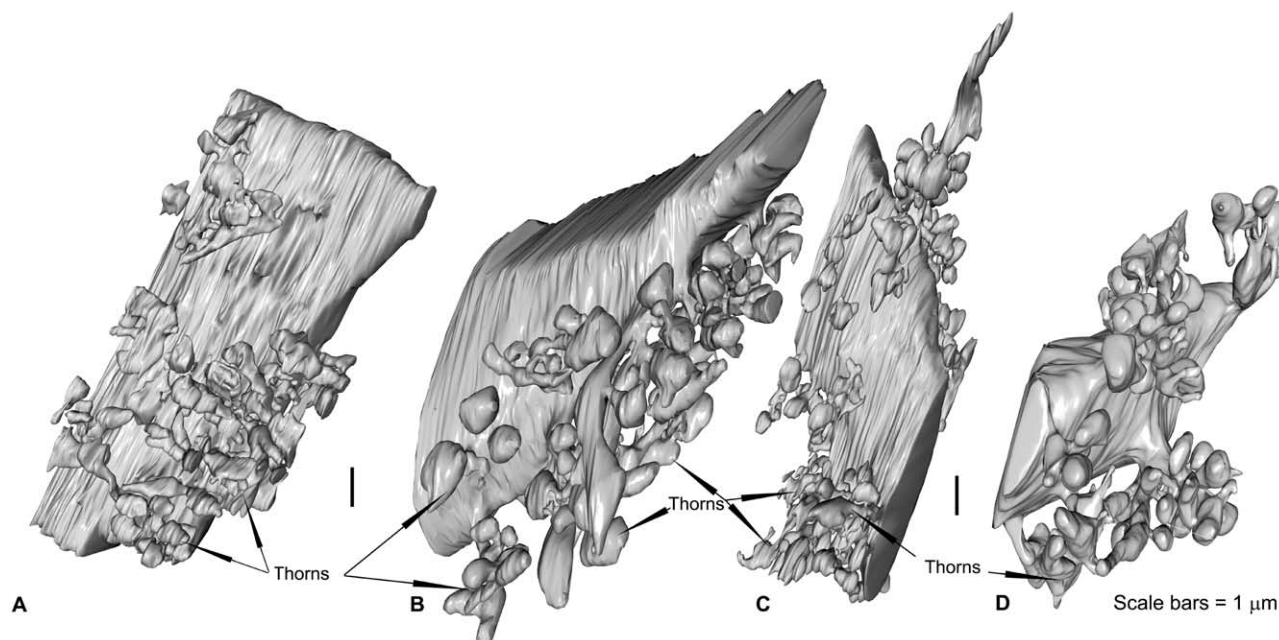


Fig. 4. (A–D) Reconstructions were made of approximately 10 dendritic segments in stratum lucidum (beginning 20 μm from the cell body) from each of the four experimental groups and representative reconstructions are shown in A–D. Qualitatively there is a distinctive and differing appearance of each of B–D compared with the dendritic segment of the control rat (A). B is from a water maze-trained rat: the dendritic shaft has increased in size and the thorns have increased in volume. C is from a restrained rat and the thorns and the dendrite have a shrunken appearance compared with that from the control rat, even though hippocampal volume has not changed overall between the two groups. In contrast following water maze training of a restrained rat (D) there has been some recovery from the shrunken state observed after restraint alone; scale bars = 1 μm .

from the cell body and otherwise chosen at random) from each of the three experimental groups and the control, and representative reconstructions are shown in Fig. 4A–D. Qualitatively there is a distinctive and differing appearance of the dendritic segment of each of three compared with that of the control rat (4A). Fig. 4B is from a water maze trained rat and the dendritic shaft appears larger with bigger thorns. However, Fig. 4C is from a restrained rat and the thorns and the dendrite have a shrunken appearance compared with that from the control rat. In contrast following water maze training of a restrained rat (Fig. 4D) there has been some recovery from the shrunken state observed after restraint alone.

These differences were confirmed by examination of the 3D structure of individual TE (Fig. 5A–D) which shows in greater detail how the thorns in the control (5A) have enlarged after water maze training (5B), retracted after restraint treatment (5C), and shown recovery to that of the control after water maze training of the restrained rats (5D). Notably, after water maze training (Fig. 5B) spinule-like protrusions appear, often connecting two thorns, but we did not attempt to quantify these.

Volume and surface area of TE. ANOVA showed that there were no significant differences for these parameters between animals within any of the four groups. However, there were significant differences between the groups. Quantitatively, measurements of the volume of the TE (Table 2) show that in the control the mean volume is 1.17 μm^3 , whilst after water maze training it has increased to 1.61 μm^3 , a 43% increase ($P < 0.005$). However, after

restraint stress the volume has decreased to 0.67 μm^3 , 57% of the control value ($P < 0.05$), but there is some recovery after water maze training of the restrained rats to 0.94 μm^3 (though these differences are not significant). In parallel the surface area of the TE increased from 10.4 μm^2 to 13.69 μm^2 ($P < 0.005$) after water maze training but fell to 5.68 μm^2 after restraint ($P < 0.05$) increasing a little to 7.69 μm^2 after water maze training of restrained rats (n.s.).

PSD parameters. Three dimensional reconstructions of examples of the two main types of PSDs of asymmetrical synapses are shown in Fig. 5E–H: these comprise (i) perforated PSDs (Fig. 5E, F) which on randomly examined 2D sections can be described as “partitioned” (Geinisman, 2000); and macular PSDs (Fig. 5G, H; Sorra and Harris, 1998; Harris, 1999; Hering and Sheng, 2001; Popov et al., 2003). PSD sizes, in terms of area and volume, were also measured in the four animal groups, as were the proportions of perforated PSDs (Table 3). An ANOVA showed that there were no significant differences for these parameters between animals within any of the four groups. The surface area of the PSDs increased significantly in all three experimental groups compared with the control ($P < 0.05$), most notably in the water maze trained group (>66%). However, the volume of the PSDs increased only after water maze training of the restraint-stressed group (>52%, $P < 0.05$). A significant increase ($P < 0.01$) in the proportion of perforated PSDs was observed following restraint stress treatment (57%) and after water maze training (240%), and also with water maze training following restraint stress (230%, $P < 0.05$).

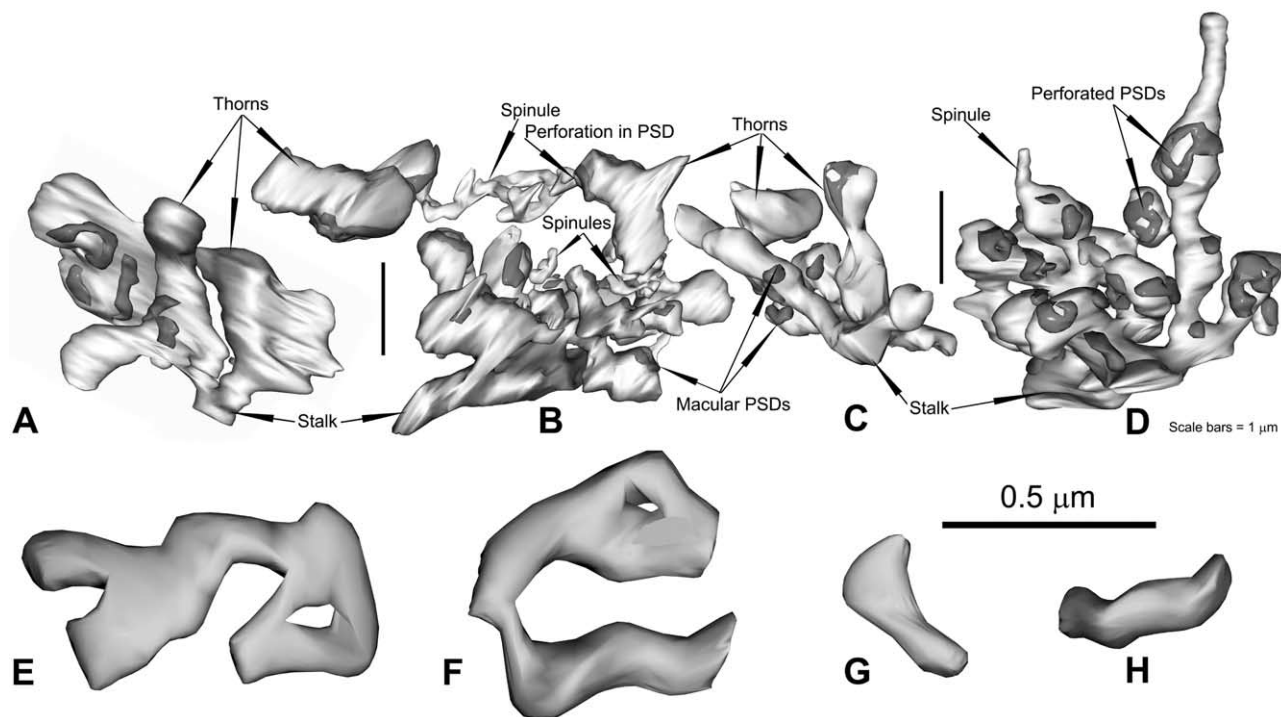


Fig. 5. A–H shows in greater detail the TE in CA3 of a control rat (A), after water maze training (B), after restraint treatment (C), and after water maze training of the restrained rats (D). Note that there is enlargement of the TE after water maze training, a decrease after restraint and partial recovery when the restrained rats have been water maze trained. Also notable in the water maze-trained rat are the presence of spinules, which project from the PSD and appear to connect two thorns; scale bar=1 μm . (E–H) 3-D reconstructions of perforated (E, F) and macular (G, H) PSDs; scale bar=0.5 μm .

Area of the TE occupied by PSDs. Because the surface areas of the TE (Table 2) have decreased following both restraint and restraint plus water maze training the area of the TE actually occupied by the PSDs which can be calculated from the ratio of these values (Table 3; divided by 2 as there are two surfaces to the PSDs). This gives an approximation of the area of the TE occupied by the PSDs and which is 12.6% in control rats, but increases to 22.7% after water maze training and to 17.9% and 18.9% after

Table 2. Quantitative parameters of 3-D reconstructions from stratum lucidum of thorny excrescences of CA3 pyramidal neurons in control and experimental animal groups^a

Animal group	The number of analyzed TE	The volume of TE in μm^3 mean \pm S.E.	The surface area of TE in μm^2 mean \pm S.E.
Control	24	1.17 \pm 0.15	10.4 \pm 1.26
Water maze	34	1.61 \pm 0.26	13.69 \pm 1.94
Restraint	56	0.67 \pm 0.11	5.68 \pm 0.74
Restraint+water maze	41	0.96 \pm 0.14	7.69 \pm 1.15

^a Data are expressed as mean of values \pm S.E. from four animals in each experimental category (three for water maze), and from each animal reconstructions were made from a minimum of 10 dendritic segments. Volume of TE: Control vs. WM, $P<0.05$; Control vs. Restraint, $P<0.05$; Control vs. Restr+WM, n.s. Surface Area of TE: Control vs. WM, $P<0.05$; Control vs. Restraint, $P<0.05$; Control vs. Restr+WM, n.s.

restraint or restraint plus water maze respectively. The validity of these figures is provided by comparison with the data of Chicurel and Harris (1992) in which the area of TE occupied by PSDs in CA3 was given as between 12 and 15% of the spine head membrane, within the range of our value for control rats.

Number of thorns and PSDs per TE. The number of thorns and PSDs per TE is shown in Table 4. In control rats the number of thorns is 5.83 and this almost doubles on water maze training to 9.56 ($P<0.01$), as was illustrated in the reconstructions in Fig. 3B and 4F. Restraint stress reduces the number slightly but not significantly and the number of thorns per TE in restraint stress rats which have been water maze trained is almost similar to that of the control animals. More significant alterations are observed in the numbers of PSDs per thorny excrescence, almost doubling from the values in control after water maze training (from 9.56 to 12.08; $P<0.01$), decreasing by 42% after restraint treatment (to 6.72; $P<0.05$) but then increasing slightly from 6.72 to 8.76 after water maze training of restrained rats (n.s.).

Number of MVBs. Measurement was made of the number of MVBs (endosome-like structures) in the TE of each of the four groups. Fig. 3E and 3F show MVBs in a control rat. MVBs were counted from the reconstructed dendritic segments and TE from each of the four animal groups. Table 5 shows that there was a significant in-

Table 3. Changes in volume and surface area of PSDs, and proportion of complicated/perforated PSDs, of TE of CA3 pyramidal in control and experimental animal groups^a

Animal group	Volume of PSD in μm^3	Surface area of PSD in μm^2	Proportion of perforated PSDs	Ratio of PSD area to TE area	Occupation by PSDs of TE surface area (%)
	mean \pm S.E.	mean \pm S.E.	mean \pm S.E.		
Control	0.0070 \pm 0.0003	0.2730 \pm 0.0084	15.5 \pm 1.0	25.1%	12.6%
Water Maze	0.0077 \pm 0.0004	0.4534 \pm 0.0174	37.5 \pm 0.9	45.36%	22.7%
Restraint	0.0072 \pm 0.0003	0.3015 \pm 0.0103	24.3 \pm 1.7	35.73	17.9%
Restraint+Water Maze	0.0107 \pm 0.0007	0.3306 \pm 0.0174	35.8 \pm 0.9	37.71	18.9%

^a Data are means of values from a minimum of 10 reconstructed dendritic segments from four animals in each group (except for water maze, three animals). A total of 1472 PSDs were analysed. Volume of PSDs: Control vs. WM and control vs. Restraint n.s.; Control vs. Restraint+WM, $P<0.05$. Surface Area of PSDs: Control vs. all groups $P<0.01$; Proportion of perforated PSDs: Control vs. WM and Restraint+WM, $P<0.01$; Control vs. Restraint, $P<0.05$.

crease in numbers of MVBs per dendritic segment from 166 to 226 after water maze training ($P<0.01$), with a reduction of approximately 30% following restraint stress ($P<0.01$) and no recovery after water maze training of the restrained animals. However, when the number of MVBs was analysed per TE, there was an increase from 3.25 to 4.83 (almost 50%) after water maze training compared with control, but a decrease to 1.66 (only 50% of control values) after restraint stress and then a small increase to 2.18 after water maze training of restraint stress rats. These differences between control and water maze and control and restraint were significant at $P<0.01$.

DISCUSSION

The present study is the first quantitative electron microscope investigation of alterations in the 3-D structure following exposure to diverse behavioural paradigms *in vivo*. Specifically, we investigated the effect of chronic stress and/or water maze training on the 3-D structure of CA3 TEs, as well as a number of morphometric parameters of PSDs originating from mossy fibres in rat hippocampus. TE represent very short branches covered by thorns, predominantly at the base of CA3 apical dendrites (Gonzales et al., 2001). We have demonstrated here that their number reflects the four different functional states of the brain examined: control, stress, water maze training, and stress

Table 4. The number thorns and PSDs per TE of CA3 pyramidal neurons in control and experimental animal groups^a

Animal group	The number of thorns per TE	The number of PSDs per TE
Control	5.83 \pm 0.40	9.56 \pm 0.84
Water maze	10.17 \pm 0.79	13.68 \pm 1.11
Restraint	4.97 \pm 0.63	6.72 \pm 1.08
Restraint+water maze	5.42 \pm 0.57	8.76 \pm 1.08

^a Data are expressed as means of values from reconstructed dendritic segments from four animals in each group (except water maze, three) \pm S.E. The number of thorns per TE: Control vs. WM, $P<0.01$; Control to both Restraint and Restraint+WM, n.s. The number of PSDs per TE: Control vs. WM, $P<0.01$; Control to both Restraint and Restraint+WM, n.s.

followed by water maze training. These results, based upon analyses of hippocampus from a new set of experimental animals, are in agreement with our preliminary findings derived from two-dimensional synaptic morphometry (Sandi et al., 2003). They therefore strongly support the view that such structural modifications could provide a neuroanatomical basis for stress-suppressing (McEwen, 1999; Kim and Diamond, 2002), and learning-inducing plasticity properties (Martin and Morris, 2002).

The data show that chronic restraint stress and spatial water maze training have a contrasting impact on CA3 dendritic and synaptic morphometry in the dorsal anterior sector of the right hippocampus. Restraint stress induces retraction of dendritic TE with a decrease in their volume, but not in the number of thorns per TE. Previous studies provided evidence highlighting apical dendrites of CA3 pyramidal neurons as particularly susceptible to the effects of sustained stress (Watanabe et al., 1992; McEwen, 1999). Reductions in length and complexity of apical, but not basal dendrites of CA3 pyramidal neurons were found using light microscopy after either chronic exposure to elevated glucocorticoid levels (Woolley et al., 1990) or to different chronic stress procedures (Watanabe et al., 1992; Magariños and McEwen, 1995; Magariños et al., 1996). The alterations in 3-D dendritic morphology we have dem-

Table 5. Quantitative analysis of MVB number (endosome-like structures) per TE of CA3 pyramidal neurons in control and experimental animal groups^a

Animal group	The number of analyzed TE	The number of analyzed MVB/endosomes per dendritic segment	The number of endosomes per TE
Control	49	166	3.25 \pm 0.32
Water maze	48	226	4.83 \pm 0.18
Restraint	71	117	1.66 \pm 0.12
Restraint+water maze	50	109	2.18 \pm 0.13

^a Data are means of values from four animals in each group (except for water maze, three animals). For each parameter: control vs. all groups; $P<0.01$.

onstrated via electron microscopy occur in more proximal regions of apical dendrites of CA3 pyramidal neurons. These are the dendritic areas receiving input from granule cells via mossy fibres (Blackstad and Kjaerheim, 1961). Our findings, therefore, reinforce the view that circuits involving synaptic contacts between mossy fibre terminals and CA3 pyramidal cells at the level of stratum lucidum are markedly affected by chronic restraint stress. Previous data has shown notable alterations in the arrangement of synaptic vesicles and synaptic mitochondrial expression in mossy fibre terminals (Magariños et al., 1997) and reduced mossy fibre-CA3 synapse density (Sousa et al., 2000; Sandi et al., 2003) following 21–28 days of stress, at the level of CA3 stratum lucidum. The possible functional relevance of these structural alterations is supported by several studies in which chronic stress resulted in impaired learning abilities in spatial learning tasks (Luine et al., 1994; Conrad et al., 1996; Venero et al., 2002; Sandi et al., 2003, 2004), as also detected here in the 'restraint plus water maze' group.

Water maze training on the other hand, increased the volume of the TE compared with that in control animals and induced increases in the proportion of perforated PSDs as well as an increase in the number of thorns per TE (Table 4), which results in increased spine complexity. Interestingly, we also observed an increase in the appearance of spinule-like protrusions, which project from the PSD and connect two thorns (Fig. 4B) but because the numbers were small, we did not quantify these. A key observation of the present study is the capacity of only two sessions of water maze training to induce, in previously restraint stressed rats, a considerable recovery in the volume of TE toward volumes found in control rats. Although the volume of the total dorsal anterior hippocampus was affected by stress with a significant reduction in volume, we did not observe any differences in overall CA3 hippocampal volume between the control and experimental groups, so our differences in spine volume can be judged to represent real differences. One caveat is that our volume measurements should be taken for relative comparisons between the four groups, since they were measured in tissue where the primary fixative was acrolein rather than glutaraldehyde so the absolute values for volumes may be slightly different than in glutaraldehyde-fixed tissue. The absence of a significant reduction in CA3 volume in stressed animals contrasts with data from Heine et al. (2004), which demonstrated a reduction in volume in CA3 (but mainly volume of the cell body layer) in chronically stressed animals. However, they found no change in volume in stratum radiatum/lucidum, in the region of hippocampus where we measured our 3-D parameters.

Our findings are supported by data from Popov et al. (1992) which used the Golgi technique to demonstrate rapid (2 h) reversibility of the retraction of CA3 TE in ground squirrels after recovery from hibernation. It is also in agreement with our previous study, where water maze training was found to rapidly revert the stress-reduced density of PSDs in TE contacted by MFB (Sandi et al., 2003). The reversibility of these structural effects of stress

was suggested previously: firstly by Sousa et al. (2000) using 2-D morphometry, which demonstrated a loss of mossy fibre-CA3 synapses following 28 days of an unpredictable multi-stress procedure, a deficit that was restored in animals allowed a recovery period of 1 month after stress exposure. Secondly, in behavioural and light microscopy studies which indicated that a period of 10–17 days from the cessation of stress exposure may be required for the reversibility of the learning impairments (Luine et al., 1994) and dendritic atrophy (Conrad et al., 1999) induced by the 21-day restraint stress procedure.

The physiological significance of the extraordinary plastic response of thorns in CA3 pyramidal cells cannot be ascertained from our data alone but we assume it reflects alterations in information processing in proximal apical dendritic segments. It is in line with mounting evidence supporting a key role for CA3 in information processing (Moser and Moser, 2003), including spatial orientation learning (Kesner et al., 2000; Steffenach et al., 2002; Stupien et al., 2003; Nakazawa et al., 2003). Training-induced increases in the volume and complexity of these spines, and of an increase in perforated PSDs in experimental groups may be related to alterations in their synaptic efficacy (Geinisman et al., 1992; Rusakov et al., 1996), which has been hypothesised to underlie memory formation (Martin and Morris, 2002). In fact, the activation properties of TE which, amongst other characteristics, display much higher EPSPs to mossy fibre inputs than those observed in activated collateral or commissural synapses, suggests a unique functional role for these synapses (Henze et al., 2000). Models of hippocampal function propose that these synapses act as 'detonator' or 'teacher' synapses, critical for directing the storage of information in the auto-associative CA3 network (McNaughton and Morris, 1987; Toth et al., 2000).

As with CA1 dendritic spines (Cooney et al., 2002), CA3 thorns contain cisterns of smooth and rER and MVBs (or endosome-like structures) originating from Golgi stacks localised in both the neuronal body and the base of CA3 apical dendrites. The observation here of an increase in endosome-like structures (similar to those seen by Cooney et al., 2002) following water maze training and a decrease following restraint stress is likely to reflect altered synaptic activity. The nature of the MVBs whose number changes remains uncertain but we know that endosomes are major sorting stations in the endocytotic route sending proteins and lipids to multiple destinations including the cell surface, Golgi complex, and lysosomes (Murk et al., 2003). Ehlers (2000) demonstrated that AMPAR sorting occurs in early endosomes and is regulated by synaptic activity and activation of AMPA and NMDA receptors, whilst Blanpied et al. (2002) showed that in dendritic spines, endocytotic zones lie lateral to the PSD where they develop and persist independent of synaptic activity, akin to the PSD itself. Steiner et al. (2002) demonstrated that in primary neurons GluR2 is internalised into endosomes and down regulation of endosomes retards recycling of GluR1 to the cell surface after NMDA stimulation. Clathrin-coated pits invaginate to form coated vesicles that become large vesicles

after the loss of the coat. Large vesicles merge into tubular endosomes and MVB-tubular complexes. Although we did not quantify endocytotic vesicles in our study, we noted qualitatively an increase in coated vesicles precisely in such a position. Cooney et al. (2002) have found that endosomal compartments were present in the head or neck of 18% of spines and were found at the origin of an additional 11% of spines. In our study, numbers of endosome-like structures were observed to increase significantly in TE, after water maze training and decrease after stress; they also altered in dendritic segments but were observed to change significantly only after water maze training, increasing by almost 30%.

In summary our data lead us to suggest that the efficacy of mossy fibre-CA3 transmission is markedly impaired by prolonged stress but can be rapidly enhanced by water maze training. The recovery in morphological structure promoted by water maze training suggests that such training experience may induce the expression of “factors” with restoring properties. The evidence available highlights neurotrophic factors (Semkova and Kriegstein, 1999) and cell recognition molecules (Kiss and Muller, 2001) as plausible candidates to mediate such recovery. Chronic restraint stress has been reported to drastically reduce the levels of neurotrophic factors (Smith 1996; Ueyama et al., 1997) as well as mRNA and protein levels of the neural cell adhesion molecule (NCAM; Sandi, 2004; Sandi et al., 2001; Venero et al., 2002; Touyarot et al., 2004). However, increased expression of neurotrophic factor (Kesslak et al., 1998; Cavallaro et al., 2002) occurs after water maze training, and manipulations interfering with expression of both neurotrophic factors (Cavallaro et al., 2002; Gorski et al., 2003) or NCAM (Arami et al., 1996; Murphy et al., 2001) have been reported to modulate spatial memory. Combined immunohistochemical and psychopharmacological studies are necessary to elucidate the potential contribution of such factors on the recovery in dendritic and synaptic structure induced by maze training. It is worth noting that both the physical activity of swimming, and spatial learning involved in water maze training are probable contributors to the recovery process, since ample evidence shows that both physical and cognitive activities can facilitate a variety of promoters and/or indexes of neural recovery (Gomez-Pinilla et al., 1998; Gould et al., 1999; Cavallaro et al., 2002; Brown et al., 2003).

Acknowledgments—M.I.C. was recipient of an FPI fellowship from the Spanish Ministry of Education and Culture (MEC), V.I.P. was supported by The Leverhulme Trust (grant F00269G) and RFBR (grants 02-04-48890a and 03-04-48747). This work was partially supported by a grant from the Ministry of Science and Technology (BF12003-07524, Spain), BBSRC 108/S08513 and BBSRC 108/NEU15416.

REFERENCES

Arami S, Jucker M, Schachner M, Welzl H (1996) The effect of continuous intraventricular infusion of L1 and NCAM antibodies on spatial learning in rats. *Behav Brain Res* 81:81–87.

- Blackstad TW, Kjaerheim (1961) Special axo-dendritic synapses in the hippocampal cortex, electron and light microscopic studies on the layer of mossy fibers. *J Comp Neurol* 117:133–159.
- Blanpied TA, Scott DB, Ehlers M (2002) Dynamics and regulation of clathrin coats at specialized endocytic zones of dendrites and spines. *Neuron* 36:435–449.
- Bliss TVP, Collingridge GL (1993) A synaptic model of memory, long-term potentiation in the hippocampus. *Nature* 361:31–39.
- Brown J, Cooper-Kuhn CM, Kempermann G, Van Praag H, Winkler J, Gage FH, Kuhn HG (2003) Enriched environment and physical activity stimulate hippocampal but not olfactory bulb neurogenesis. *Eur J Neurosci* 17:2042–2046.
- Cavallaro SD, Agata V, Manickam P, Dufour F, Alkon DL (2002) Memory-specific temporal profiles of gene expression in the hippocampus. *Proc Natl Acad Sci USA* 99:16279–16284.
- Chicurel ME, Harris KM (1992) Three-dimensional analysis of the structure and composition of CA3 branched dendritic spines and their synaptic relationships with mossy fiber boutons in the rat hippocampus. *J Comp Neurol* 325:169–182.
- Conrad CD, Galea LAM, Kuroda Y, McEwen BS (1996) Chronic stress impairs rat spatial memory on the Y maze and this effect is blocked by tianeptine pre-treatment. *Behav Neurosci* 110:1321–1334.
- Conrad CD, LeDoux JE, Magariños AM, McEwen BS (1999) Repeated restraint stress facilitates fear conditioning independently of causing hippocampal CA3 dendritic atrophy. *Behav Neurosci* 113:902–913.
- Cooney JR, Hurlburt JL, Selig DK, Harris KM, Fiala JC (2002) Endosomal compartments serve multiple hippocampal dendritic spines from a widespread rather than a local store of recycling membrane. *J Neurosci* 22:2215–2224.
- Cordero MI, Krutik ND, Sandi C (2003) Modulation of contextual fear conditioning by chronic stress in rats is related to individual differences in behavioral reactivity to novelty. *Brain Res* 970:242–245.
- de Kloet ER, Vreugdenhil E, Oitzl MS, Joëls M (1998) Brain corticosteroid receptor balance in health and disease. *Endocr Rev* 19:269–301.
- Ehlers MD (2000) Reinsertion or degradation of AMPA receptors determined by activity-dependent endocytic sorting. *Neuron* 28:511–525.
- Engert F, Bonhoeffer T (1999) Dendritic spine changes associated with hippocampal long-term synaptic plasticity. *Nature* 399:66–70.
- Eyre MD, Richter-Levin G, Avital A, Stewart MG (2003) Morphological changes in hippocampal synapses following spatial learning in rats are transient. *Eur J Neurosci* 17:1973–1980.
- Fiala JC, Harris KM (2001) Extending unbiased stereology of brain ultrastructure to three-dimensional volumes. *J Am Med Inform Assoc* 8:1–16.
- Fuchs E, Flugge G, Ohl F, Lucassen P, Vollmann-Honsdorf GK, Michaelis T (2001) Psychosocial stress, glucocorticoids, and structural alterations in the tree shrew hippocampus. *Physiol Behav* 73:285–291.
- Geinisman Y, de Toledo-Morrell L, Morrell F, Persina IS, Rossi M (1992) Structural synaptic plasticity associated with the induction of long-term potentiation is preserved in the dentate gyrus of aged rats. *Hippocampus* 2:445–456.
- Geinisman Y (2000) Structural synaptic modifications associated with hippocampal LTP and behavioral learning. *Cereb Cortex* 10:952–962.
- Gomez-Pinilla F, So V, Kesslak JP (1998) Spatial learning and physical activity contribute to the induction of fibroblast growth factor, neural substrates for increased cognition associated with exercise. *Neuroscience* 85:53–61.
- Gonzales RB, DeLeon Galvin C, Rancel YM, Clairborne BJ (2001) Distribution of thorny excrescences on CA3 pyramidal neurons in rat hippocampus. *J Comp Neurol* 430:357–368.
- Gorski JA, Balogh SA, Wehner JM, Jones KR (2003) Learning deficits in forebrain-restricted brain-derived neurotrophic factor mutant mice. *Neuroscience* 121:341–354.

- Gould E, Beylin A, Tanapat P, Reeves A, Shors TJ (1999) Learning enhances adult neurogenesis in the hippocampal formation. *Nat Neurosci* 2:260–265.
- Harris KM (1999) Structure, development, and plasticity of dendritic spines. *Curr Opin Neurobiol* 9:343–348.
- Harris KM, Fiala JC, Ostroff L (2003) Structural changes at dendritic spine synapses during long-term potentiation. *Philos Trans R Soc Lond B Biol Sci* 358:745–748.
- Henze DA, Urban NN, Barrionuevo G (2000) The multifarious hippocampal mossy fiber pathway, a review. *Neuroscience* 98:407–427.
- Heine VM, Maslam S, Zareno J, Joels M, Lucassen PJ (2004) Suppressed proliferation and apoptotic changes in the rat dentate gyrus after acute and chronic stress are reversible. *Eur J Neurosci* 19:131–144.
- Hering H, Sheng M (2001) Dendritic spines: structure, dynamics and regulation. *Nat Rev Neurosci* 2:880–888.
- Jung MW, Wiener SI, McNaughton BL (1994) Comparison of spatial firing characteristics of units in dorsal and ventral hippocampus of the rat. *J Neurosci* 14:7347–7356.
- Kesslak JP, So V, Choi J, Cotman CW, Gomez-Pinilla F (1998) Learning upregulates brain derived neurotrophic factor messenger ribonucleic acid: a mechanism to facilitate encoding and circuit maintenance. *Behav Neurosci* 112(4):1012–1019.
- Kesner RP, Gilbert PE, Wallenstein GV (2000) Testing neural network models of memory with behavioral experiments. *Curr Opin Neurobiol* 10:260–265.
- Kim JJ, Diamond DM (2002) The stressed hippocampus, synaptic plasticity and lost memories. *Nat Rev Neurosci* 3:453–462.
- Kiss JZ, Muller D (2001) Contribution of the neural cell adhesion molecule to neuronal and synaptic plasticity. *Rev Neurosci* 12:297–310.
- Luine V, Villegas M, Martínez C, McEwen BS (1994) Repeated stress causes reversible impairments of spatial memory performance. *Brain Res* 639:167–170.
- Magariños AM, McEwen BS (1995) Stress-induced atrophy of apical dendrites of hippocampal CA3c neurons, comparison of stressors. *Neuroscience* 69:83–88.
- Magariños AM, McEwen BS, Flugge G, Fuchs E (1996) Chronic psychosocial stress causes apical dendritic atrophy of hippocampal CA3 pyramidal neurons in subordinate tree shrews. *J Neurosci* 16:3534–3540.
- Magariños AM, García-Verdugo JM, McEwen BS (1997) Chronic stress alters synaptic terminal structure in the hippocampus. *Proc Natl Acad Sci USA* 94:14002–14008.
- Martin SJ, Morris RGM (2002) New life in an old idea, the synaptic plasticity and memory hypothesis revisited. *Hippocampus* 12:609–636.
- McEwen BS (1999) Stress and hippocampal plasticity. *Annu Rev Neurosci* 22:105–122.
- McNaughton N, Morris RG (1987) Chlordiazepoxide, an anxiolytic benzodiazepine, impairs place navigation in rats. *Behav Brain Res* 24:39–46.
- Mezey S, Doyère V, Souza I, Harrison E, Cambon C, Kendal CE, Davies HA, Laroche S, Stewart MG (2004) Long-term synaptic morphometry changes after induction of LTP and LTD in the dentate gyrus of awake rats are not simply mirror phenomena. *Eur J Neurosci* 19:2310–2318.
- Morris RG, Garrud P, Rawlins JN, O'Keefe J (1982) Place navigation impaired in rats with hippocampal lesions. *Nature* 297:681–683.
- Moser E, Moser MB, Andersen P (1993) Spatial-learning impairment parallels the magnitude of dorsal hippocampal-lesions, but is hardly present following ventral lesions. *J Neurosci* 13:3916–3925.
- Moser MB, Trommald M, Andersen P (1994) An increase in dendritic spine density on hippocampal CA1 pyramidal cells following spatial learning in adult rats suggests the formation of new synapses. *Proc Natl Acad Sci USA* 91:12673–12675.
- Moser MB, Moser EI, Forrest E, Andersen P, Morris RGM (1995) Spatial learning with minilab in the dorsal hippocampus. *Proc Natl Acad Sci USA* 92:9697–9701.
- Moser MB, Trommald M, Egeland T, Andersen P (1997) Spatial training in a complex environment and isolation alter the spine distribution differently in rat CA1 pyramidal cells. *J Comp Neurol* 380:373–381.
- Moser EI, Moser MB (2003) One-shot memory in hippocampal CA3 networks. *Neuron* 38:147–148.
- Muller D, Nikonenko I (2003) Dynamic presynaptic varicosities: a role in activity-dependent synaptogenesis. *Trends Neurosci* 26:573–575.
- Murk JL, Humbel BM, Ziese U, Griffith JM, Posthuma G, Slot JW, Koster AJ, Verkleij AJ, Geuze HJ, Kleijmeer MJ (2003) Endosomal compartmentalization in three dimensions: implications for membrane fusion. *Proc Natl Acad Sci USA* 100:13332–13337.
- Murphy KJ, Fox GB, Foley AG, Gallagher HC, O'Connell A, Griffin AM, Nau H, Regan CM (2001) Pentylenetetrazol enhances both spatial and avoidance learning, and attenuates age-related NCAM-mediated neuroplastic decline within the rat medial temporal lobe. *J Neurochem* 78:704–714.
- Nakazawa K, Sun LD, Quirk MC, Rondi-Reig L, Wilson MA, Tonegawa S (2003) Hippocampal CA3 NMDA receptors are crucial for memory acquisition of one-time experience. *Neuron* 38:305–315.
- Nikonenko I, Jourdain P, Alberi S, Toni N, Muller D (2002) Activity-induced changes of spine morphology. *Hippocampus* 12:585–591.
- O'Keefe J, Nadel L (1978) *The hippocampus as a cognitive map*. Oxford: Clarendon.
- O'Malley A, O'Connell C, Murphy KJ, Regan CM (2000) Transient spine density increases in the mid-molecular layer of hippocampal dentate gyrus accompany consolidation of a spatial learning task in the rodent. *Neuroscience* 99:229–232.
- Pakkenberg B, Gundersen HJ (1997) Neocortical neuron number in humans: effect of sex and age. *J Comp Neurol* 384:312–320.
- Popov VI, Bocharova LS, Bragin AG (1992) Repeated changes of dendritic morphology in the hippocampus of ground squirrels in the course of hibernation. *Neuroscience* 48:45–51.
- Popov VI, Medvedev NI, Rogachevskii VV, Ignat'ev DA, Stewart MG, Fesenko EE (2003) Three-dimensional organization of synapses and astroglia in the hippocampus of rats and ground squirrels: new structural and functional paradigms of the synapse function. *Biofizika* 48:289–308.
- Popov VI, Davies HA, Rogachevskii VV, Patrushev IV, Errington ML, Gabbott PLA, Bliss TVP, Stewart MG (2004) Remodelling of synaptic morphology but unchanged synaptic density during late phase LTP: a serial section EM study of the dentate gyrus in the anaesthetized rat. *Neuroscience* 28:251–262.
- Ramírez-Amaya V, Escobar ML, Chao V, Bermúdez-Rattoni F (1999) Synaptogenesis of mossy fibers induced by spatial water maze overtraining. *Hippocampus* 9:631–636.
- Ramírez-Amaya V, Balderas I, Sandoval J, Escobar ML, Bermúdez-Rattoni F (2001) Spatial long-term memory is related to mossy fiber synaptogenesis. *J Neurosci* 21:7340–7348.
- Ramón y Cajal S (1911) *Histologie du système nerveux de l'homme et des vertébrés: tome II*. Paris: Maloine.
- Reynolds ES (1963) The use of lead citrate at high pH as an electron-opaque stain in electron microscopy. *J Cell Biol* 17:208–212.
- Riedel G, Micheau J, Lam AG, Roloff E, Martin SJ, Bridge H, Hoz L, Poeschel B, McCulloch J, Morris G (1999) Reversible neural inactivation reveals hippocampal participation in several memory processes. *Nat Neurosci* 2:898–905.
- Rusakov D, Stewart MG, Korogod SM (1996) Branching of active dendritic spines as a mechanism for controlling synaptic efficacy. *Neurosci* 75:315–323.
- Sandi C (2004) Stress, cognitive impairment and cell adhesion molecules. *Nat Rev Neurosci* 5:917–930.
- Sandi C, Merino JJ, Cordero MI, Touyarot K, Venero C (2001) Effects of chronic stress on contextual fear conditioning and the hip-

- pocampal expression of the neural cell adhesion molecule, its polysialylation, and L1. *Neuroscience* 102:329–339.
- Sandi C, Davies HA, Cordero MI, Rodriguez JJ, Popov VI, Stewart MG (2003) Rapid reversal of stress induced loss of synapses in CA3 of rat hippocampus following water maze training. *Eur J Neurosci* 17:2447–2456.
- Semkova I, Kriegstein J (1999) Neuroprotection mediated via neurotrophic factors and induction of neurotrophic factors. *Brain Res Rev* 30:176–188.
- Smith MA (1996) Hippocampal vulnerability to stress and aging: possible role of neurotrophic factors. *Behav Brain Res* 78:25–36.
- Sorra KE, Harris KM (1998) Stability in synapse number and size at 2 hr after long-term potentiation in hippocampal area CA1. *J Neurosci* 15:658–671.
- Sousa N, Lukoyanov NV, Madeira MD, Almeida OFX, Paula-Barbosa MM (2000) Reorganization of the morphology of hippocampal neurites and synapses after stress-induced damage correlates with behavioral improvement. *Neuroscience* 97:253–266.
- Steffenach H-A, Sloviter RS, Moser EI, Moser MB (2002) Impaired retention of spatial memory after transection of longitudinally oriented axons of hippocampal CA3 pyramidal cells. *Proc Natl Acad Sci USA* 99:3194–3198.
- Steiner P, Sarria JC, Glauser L, Magnin S, Catsicas S, Hirling H (2002) Modulation of receptor cycling by neuron-enriched endosomal protein of 21 kD. *J Cell Biol* 157:1197–1209.
- Sterio DC (1984) The unbiased estimation of the number and sizes of arbitrary particles using the disector. *J Microsc* 134:127–136.
- Stewart MG, Harrison E, Rusakov DA, Richter-Levin G, Maroun M (2000) Re-structuring of synapses 24 hours after induction of long-term potentiation in the dentate gyrus of the rat hippocampus in vivo. *Neuroscience* 100:221–227.
- Stuart DA, Oorschot DE (1995) Embedding, sectioning, immunocytochemical and stereological methods that optimise research on the lesioned adult rat spinal cord. *J Neurosci Methods* 61:5–14.
- Stupien G, Florian C, Roulet P (2003) Involvement of the hippocampal CA3-region in acquisition and in memory consolidation of spatial but not in object information in mice. *Neurobiol Learn Mem* 80:32–41.
- Swanson LW (1998) *Brain maps: structure of the rat brain*. Amsterdam: Elsevier.
- Toth K, Soares G, Lawrence JJ, Philips-Tansey E, McBain CJ (2000) Differential mechanisms of transmission at three types of mossy fiber synapse. *J Neurosci* 20:8279–8289.
- Touyarot K, Venero C, Sandi C (2004) Spatial learning impairment induced by chronic stress is related to individual differences in novelty reactivity, search for neurobiological correlates. *Psychoneuroendocrinology* 29:290–305.
- Ueyama T, Kawai Y, Nemoto K, Sekimoto M, Tone S, Senba E (1997) Immobilization stress reduced the expression of neurotrophins and their receptors in the rat brain. *Neurosci Res* 28:103–110.
- Venero C, Tilling T, Hermans-Borgmeyer I, Schmidt R, Schachner M, Sandi C (2002) Chronic stress induces opposite changes in the mRNA expression of the neural cell adhesion molecules NCAM and L1. *Neuroscience* 115:1211–1219.
- Watanabe Y, Gould E, McEwen BS (1992) Stress induces atrophy of apical dendrites of hippocampal CA3 pyramidal neurons. *Brain Res* 588:341–345.
- Woolley CS, Gould E, McEwen BS (1990) Exposure to excess glucocorticoids alters dendritic morphology of adult hippocampal pyramidal neurons. *Brain Res* 531:225–231.

(Accepted 28 October 2004)
(Available online 24 December 2004)